

QCD phase diagram at finite baryon and isospin chemical potentials in Polyakov loop extended quark meson model with vector interaction

H. Ueda,^{1,2} T. Z. Nakano,^{1,2} A. Ohnishi,² M. Ruggieri,³ and K. Sumiyoshi⁴

¹*Department of Physics, Faculty of Science, Kyoto University, Kyoto 606-8502, Japan*

²*Yukawa Institute for Theoretical Physics, Kyoto University, Kyoto 606-8502, Japan*

³*Department of Physics and Astronomy, University of Catania, Via S. Sofia 64, I-95125 Catania, Italy*

⁴*Numazu College of Technology, Ooka 3600, Numazu, Shizuoka 410-8501, Japan*

We investigate the QCD phase diagram of isospin asymmetric matter using the Polyakov loop extended quark meson (PQM) model with vector interaction. The critical point temperature is found to decrease in isospin asymmetric matter and disappear at large isospin chemical potential. We also discuss the QCD phase transition in the neutron star core. From comparison of the QCD phase diagram in PQM and corresponding baryon and isospin chemical potentials of neutron star matter in relativistic mean field models, we show that the order of the chiral phase transition in the neutron star core could be crossover because of large isospin chemical potential.

PACS numbers: 12.38.Lg, 21.65.Qr

I. INTRODUCTION

The QCD phase transition would be realized not only in heavy-ion collisions but also in compact astrophysical objects and phenomena such as heavy neutron stars [1], supernovae [2] and black hole formations [3–6]. At zero baryon chemical potential (μ_B), the QCD phase transition at finite temperature (T) is accessible by using the lattice Monte Carlo simulation, e.g. [7, 8]. At large μ_B , $\mu_B/T \gtrsim 1$, the situation is much less clear since the lattice simulation is plagued by the well-known sign problem [9]. We can investigate this region by using chiral effective models such as the Nambu–Jona-Lasinio (NJL) model [10] and the quark meson (QM) model [11], and the chiral effective model with the Polyakov loop effects such as the Polyakov loop extended Nambu–Jona-Lasinio (PNJL) model [12–14] and the Polyakov loop extended quark meson (PQM) model [15, 16]. The QCD phase diagram, especially the QCD critical point (CP) location, strongly depends on models and model parameters [17]. Therefore, further experimental and theoretical developments are necessary to determine the structure of the QCD phase diagram.

For laboratory experiments, the search for CP in heavy-ion collisions is ongoing at RHIC [18] and is planned in the coming FAIR facility. Since the phase transition is second order at CP, the coherence length ξ is divergent and large fluctuations of the order parameter are expected in a volume of the size ξ^3 . Various signatures of CP have been proposed theoretically [19]. It is not an easy task to observe the divergence signature of ξ in heavy-ion collisions, since the system size and the evolution time are limited. Moreover, it is difficult to create cold dense matter, and CP may not be reachable in the laboratory if CP is located in the high density region, $\mu_B > 500$ MeV.

By comparison, very dense matter is formed in compact astrophysical phenomena. For example, high density and low temperature matter is formed in the neutron star core, and high temperature and high density matter is produced during a gravitational collapse of a massive star and binary stars [20]. From the observation of these phenomena, we

may get information on the QCD phase diagram in the high density region [1–6]. In compact astrophysical phenomena, charge neutrality leads to suppressed proton fraction compared with that of neutrons, and the isospin chemical potential $\delta\mu \equiv (\mu_n - \mu_p)/2 = (\mu_d - \mu_u)/2$ is finite and positive. In particular, $\delta\mu$ appears as another independent thermodynamical variable in supernovae and BH formations, since trapped neutrinos modify the neutrinoless charge neutrality condition ($\delta\mu = \mu_e/2$). Therefore it is necessary to consider $\delta\mu$ dependence of the QCD phase diagram in order to discuss the QCD phase transition in compact star phenomena.

The phase structure in the three thermodynamic variables ($T, \mu, \delta\mu$) is still an open problem. In our previous work [6], we have discussed the possibility of the CP sweep during BH formation processes where $\delta\mu$ is finite; quark matter core and hadronic envelope may merge to one phase, when the temperature exceeds the CP temperature (T_{CP}). The location of CP strongly depends on $\delta\mu$; for large $\delta\mu$, T_{CP} becomes lower and it becomes more probable for the heated matter to go through CP. There are several recent works which discuss the QCD phase diagram in charge neutral dense matter [21] and in the three-dimensional space, ($T, \mu, \delta\mu$) [22, 23] or (T, μ, μ_L) [24], where μ_L is the lepton-number chemical potential. The phase diagram structures in these works have some differences. In Ref. [21], the isospin chemical potential is found to be small $\delta\mu < m_\pi/2$ in charge neutral quark matter, and pions are not found to condense. In Ref. [22], three-dimensional ($T, \mu, \delta\mu$) phase diagram is investigated in the mean-field approximation, and the s -wave pion condensed phase is found to appear in the finite μ and $\delta\mu$ region. T_{CP} decreases with increasing $\delta\mu$, until the CP hits the pion condensation phase boundary. In Ref. [23], fluctuation effects are taken into account in the quark meson model by using the functional renormalization group (FRG) flow equation. T_{CP} is also found to decrease with increasing $\delta\mu$. The s -wave pion condensed phase is found in the high $\delta\mu$ and low μ region, but it is suppressed at large μ . As a result, the pion condensed phase is separated from the chiral first order phase transition surface in the ($T, \mu, \delta\mu$) space. In Ref. [24], T_{CP} is found to be insensitive to the lepton-number chemical potential.

In this article, we investigate the isospin chemical potential dependence of the QCD phase diagram in more detail, and discuss the order of the chiral phase transition in the neutron star core, where $T = 0$ and $\mu_B, \delta\mu > 0$. For this purpose, we first compute the QCD phase diagram using the two-flavor PQM with vector interaction and examine the $\delta\mu$ dependence of the QCD phase diagram. According to the s -wave πN repulsion argument [25] and functional renormalization group results [23], we assume that pions do not condensate. We then discuss the order of the chiral phase transition in neutron star core, through the comparison of the QCD phase diagram with the β equilibrium line in neutron star matter calculated by using hadronic equation of states (EOSs).

The article is organized as follows: In Sec.II, we briefly describe PQM with vector interaction. The results are discussed in Sec.III, where we show the $\delta\mu$ dependence of the QCD phase diagram and compare the QCD phase diagram in PQM with neutron star matter chemical potentials. Sec.IV is devoted to summary and discussion.

II. POLYAKOV LOOP EXTENDED QUARK MESON MODEL

A. PQM Lagrangian and parameters

In this Section, we describe the PQM model augmented with the vector interaction. PQM is an effective model which has the chiral symmetry and confinement property of QCD [15, 16]. The Lagrangian density of the two-flavor PQM is given by [15, 16]

$$\begin{aligned} \mathcal{L} = & \bar{q} [i\gamma^\mu D_\mu - g(\sigma + i\gamma_5 \boldsymbol{\tau} \cdot \boldsymbol{\pi}) - g_\omega \gamma^\mu \omega_\mu - g_\rho \gamma^\mu \boldsymbol{\tau} \cdot \mathbf{R}_\mu] q \\ & + \frac{1}{2}(\partial_\mu \sigma)^2 + \frac{1}{2}(\partial_\mu \boldsymbol{\pi})^2 - U(\sigma, \boldsymbol{\pi}) \\ & - \frac{1}{4}\omega_{\mu\nu}\omega^{\mu\nu} - \frac{1}{4}\mathbf{R}_{\mu\nu} \cdot \mathbf{R}^{\mu\nu} + \frac{1}{2}m_v^2(\omega_\mu\omega^\mu + \mathbf{R}_\mu \cdot \mathbf{R}^\mu) \\ & - \mathcal{U}(P, \bar{P}, T), \end{aligned} \quad (1)$$

where q denotes a quark field with Dirac, color and flavor indices, $\boldsymbol{\tau}$ is the Pauli matrix in the flavor space and $\omega^{\mu\nu}$ and $\mathbf{R}^{\mu\nu}$ are the field tensors of ω and ρ mesons. The mesonic potential U and the Polyakov loop potential \mathcal{U} are given as,

$$U(\sigma, \boldsymbol{\pi}) = \lambda(\sigma^2 + \boldsymbol{\pi}^2 - v^2)^2/4 - h\sigma, \quad (2)$$

$$\mathcal{U}[P, \bar{P}, T] = T^4 \left\{ -\frac{a(T)}{2} \bar{P}P + b(T) \ln H(P, \bar{P}) \right\}, \quad (3)$$

$$H(P, \bar{P}) = 1 - 6\bar{P}P + 4(\bar{P}^3 + P^3) - 3(\bar{P}P)^2. \quad (4)$$

σ and $\boldsymbol{\pi}$ are the isoscalar-scalar and isovector-pseudoscalar meson fields. The covariant derivative $D_\mu = \partial_\mu - iA_\mu$ in Eq. (1) is the Dirac operator with a temporal static and homogeneous background gluon field $A_\mu = \delta_{\mu 0}A_0$. Without the explicit symmetry breaking term, the last term in Eq. (2), the Lagrangian in Eq. (1) has $SU(2)_L \times SU(2)_R$ symmetry.

$\mathcal{U}(P, \bar{P}, T)$ is an effective potential of gluon field, where P

and \bar{P} are the Polyakov loop and its conjugate,

$$P = \frac{1}{N_c} \text{Tr} L, \quad \bar{P} = \frac{1}{N_c} \text{Tr} L^\dagger. \quad (5)$$

L is defined in the Euclidean space as,

$$L = \mathcal{P} \exp \left(i \int_0^\beta d\tau A_4 \right), \quad (6)$$

where \mathcal{P} stands for the path ordering. The logarithmic term $\ln H(P, \bar{P})$ in Eq. (3) comes from the Haar measure of the group integral in strong-coupling lattice QCD [13]. Coefficients, $a(T)$ and $b(T)$, are given as functions of T , and parameterized as $a(T) = a_0 + a_1(T_0/T) + a_2(T_0/T)^2$, and $b(T) = b_3(T_0/T)^3$ [14].

B. Effective Potential

We now give the effective potential in dense asymmetric matter in PQM. In asymmetric matter, u and d quark populations are unbalanced, and we need to introduce two independent chemical potential for u and d quarks

$$\mu_u = \mu - \delta\mu, \quad \mu_d = \mu + \delta\mu, \quad (7)$$

where $\mu = \mu_B/3$ is the quark chemical potential. The isospin chemical potential $\delta\mu$ is an independent thermodynamical variable in supernovae or black hole formation processes, while the neutrino-less β -equilibrium condition, $\delta\mu = \mu_e/2$, applies to cold neutron star matter.

We assume that the σ meson and the temporal components of ω and ρ^0 mesons take finite expectation values, while others do not. These expected values are assumed to be constant. In this approximation, the quark single-quasiparticle energy is given by

$$E_{fp}^* = E_p + g_\omega \omega + g_\rho \tau^3 R, \quad (8)$$

with

$$E_p = \sqrt{\mathbf{p}^2 + M^2}, \quad M = g\sigma. \quad (9)$$

ω and R in Eq. (8) denote the expectation values of ω and ρ^0 mesons ($\omega = \langle \omega_0 \rangle, R = \langle R_0^3 \rangle$), respectively, where the subscript 0 denotes the temporal component and the superscript 0 shows isospin. The effect of vector interaction is to shift the quark chemical potential [26]. For later convenience, we define effective chemical potentials for u and d quarks,

$$\tilde{\mu}_u = \mu - \delta\mu - g_\omega \omega - g_\rho R, \quad \tilde{\mu}_d = \mu + \delta\mu - g_\omega \omega + g_\rho R. \quad (10)$$

Integrating over the quark fields results in the following effective

tive potential,

$$\Omega_{PQM} = \mathcal{U}(P, \bar{P}, T) + U(\sigma, \pi = 0) + \Omega_0 + \Omega_T, \quad (11)$$

$$\Omega_0 = -2N_f N_c \int \frac{d\mathbf{p}}{(2\pi)^3} E_p \theta(\Lambda^2 - \mathbf{p}^2), \quad (12)$$

$$\Omega_T = -\frac{1}{2} (m_\omega^2 \omega^2 + m_\rho^2 R^2) - 2T \sum_f \int \frac{d\mathbf{p}}{(2\pi)^3} \log(F_-^f F_+^f), \quad (13)$$

$$F_-^f = 1 + 3P e^{-\beta \mathcal{E}_-^f} + 3\bar{P} e^{-2\beta \mathcal{E}_-^f} + e^{-3\beta \mathcal{E}_-^f}, \quad (14)$$

$$F_+^f = 1 + 3\bar{P} e^{-\beta \mathcal{E}_+^f} + 3P e^{-2\beta \mathcal{E}_+^f} + e^{-3\beta \mathcal{E}_+^f}, \quad (15)$$

$$\mathcal{E}_\pm^f = E_p \pm \tilde{\mu}_f, \quad (16)$$

where Ω_T is the thermal contribution and Ω_0 is the fermion vacuum energy, regularized by the ultraviolet cutoff Λ . This term is necessary to reproduce the second-order chiral phase transition at zero baryon chemical potential μ_B in the chiral limit [16]. Each term on the right hand side of Eq. (14) corresponds to the thermal contribution of zero, one, two, and three quark states. Similarly, Eq. (15) is the thermal contribution of antiquarks. While PQM is renormalizable and we can use dimensional renormalization [16], it is sufficient to cut large momenta by a hard cutoff for our purposes.

The equations of motion are obtained from the stationary conditions in equilibrium,

$$\frac{\partial \Omega}{\partial \sigma} = \frac{\partial \Omega}{\partial P} = \frac{\partial \Omega}{\partial \bar{P}} = \frac{\partial \Omega}{\partial \omega} = \frac{\partial \Omega}{\partial R} = 0. \quad (17)$$

We obtain $(T, \mu_B, \delta\mu)$ dependence of the mean fields, $\sigma, P, \bar{P}, \omega$ and R , by solving these equations.

Here we do not consider the pion condensation because the s-wave pion condensation will not occur in neutron stars when we take account of the s-wave πN repulsion [25]. Functional renormalization group analysis also shows the shrinkage of the pion condensed region at finite μ than naively expected ($\delta\mu > m_\pi/2$) [23].

C. Model parametrization

The parameter in the scalar-pseudoscalar part, g, λ, ν, h are fixed to reproduce some properties of quarks and mesons in vacuum for a given value of the hard momentum cut off $\Lambda = 600$ MeV in this work. The quark-scalar meson coupling g is determined by the constituent quark mass in the vacuum $m_q = g\sigma = 335$ MeV. The mesonic potential parameters λ and ν are given by the chiral condensate in the vacuum $\sigma = f_\pi = 92.4$ MeV, and the σ meson mass $m_\sigma^2 = \partial^2 \Omega / \partial \sigma^2 = (700 \text{ MeV})^2$. The explicit symmetry breaking parameter h is given by the pion mass $h = m_\pi^2 f_\pi$.

In this study, we assume the quark-vector couplings are the same ($g_\omega = g_\rho = g_v$) for simplicity. We regard g_v as a free parameter, and we compare the results with several values of $r = g_v/g$. We also assume the common vector meson masses ($m_\omega = m_\rho = m_v = 770$ MeV)

The parameters in the Polyakov loop potential are fitted to the pure gauge lattice data [27]. The standard choice of the parameters reads [14] $a_0 = 3.51, a_1 = -2.47, a_2 = 15.2$ and $b_3 = -1.75$. The parameter T_0 in Eq. (3) sets the deconfinement scale in the pure gauge theory, i.e. $T_0 = 270$ MeV. Chemical potential dependence of these parameters is not considered in this work [15, 28].

III. RESULTS

In this section, we discuss the $\delta\mu$ and the vector coupling dependence of the QCD phase diagram. The chiral phase transition is found to be weakened at finite $\delta\mu$ or with finite vector coupling r . In order to demonstrate this point, we first discuss the order parameters as functions of μ_B at several values of $\delta\mu$ and r .

The phase structure is obtained from the behavior of the order parameters σ, P and \bar{P} . Figure 1 shows μ_B dependence of the order parameters, σ (left) and P (right), for several isospin chemical potentials at $T = 96.5$ MeV $= T_{CP}(\delta\mu = 50 \text{ MeV}, r = 0)$ (CP temperature at $\delta\mu = 50$ MeV and the vector-scalar coupling ratio $r = 0$). For small $\delta\mu$, the chiral phase transition is first-order, while for $\delta\mu \gtrsim 50$ MeV, the chiral phase transition becomes crossover. The change of the nature of the phase transition with the increase of $\delta\mu$ is not a peculiarity of the PQM model; in fact, several chiral models share this property, as discussed in [6] (see also the Appendix for a discussion within the NJL model).

In Fig. 2, we show σ (left) and P (right) as functions of the baryon chemical potential at $T = 101.5$ MeV $= T_{CP}(\delta\mu = 0, r = 0.2)$ and $\delta\mu = 0$ MeV for several values of the vector-scalar coupling ratio r . For the strong vector interaction, the transition chemical potential is shifted to higher values, and the chiral phase transition is smoothed. The transition becomes crossover for $r \gtrsim 0.2$ at this T .

We next discuss the $\delta\mu$ and vector coupling dependence of the chiral and deconfinement phase boundaries. Since the chiral phase transition at small μ_B is actually a smooth crossover for finite quark masses, we have to establish a criterion to identify the phase boundary of the chiral transition. Here we define the chiral critical temperature T_c or the baryon chemical potential $\mu_{B,c}$ of the chiral phase transition by the peak of the chiral susceptibility χ_σ as a function of T or μ_B for fixed $\delta\mu$ and μ_B or T , respectively. Since χ_σ is divergent at the critical point, we can unambiguously determine the critical point temperature T_{CP} and baryon chemical potential μ_{CP} by the diverging peak of χ_σ in the $T - \mu_B$ plane. The chiral susceptibility is defined as the second derivative of the effective potential by the explicit chiral breaking coefficient h ,

$$\chi_\sigma = -T^3 \frac{\partial^2 (\Omega/T)}{\partial h^2}. \quad (18)$$

Since $h \propto m_\pi^2$ is proportional to the bare quark mass, the above definition gives a susceptibility which is proportional to the usual definition around the critical point, $\chi_\sigma = -\partial^2 \Omega / \partial M^2 / T^2$, where M is the bare quark mass. We normalize Eqs. (18) by multiplying some powers of T to con-

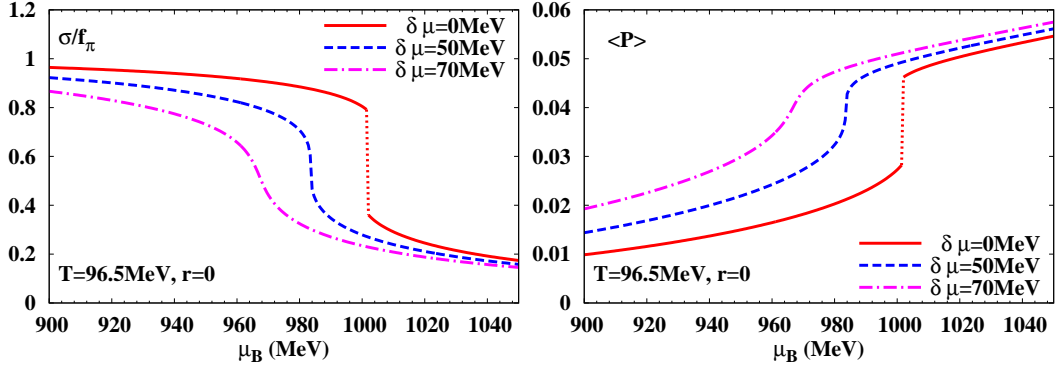


FIG. 1. The order parameters σ (left panel), P (right panel) as functions of baryon chemical potential μ_B at $T = 96.5 \text{ MeV} = T_{CP}(\delta\mu = 50 \text{ MeV}, r = 0)$ and three different isospin chemical potentials $\delta\mu = 0$ (solid line), 50 (dash line), 70 MeV (dash-dot line). The vector-scalar coupling ratio is chosen to be $r = 0$.

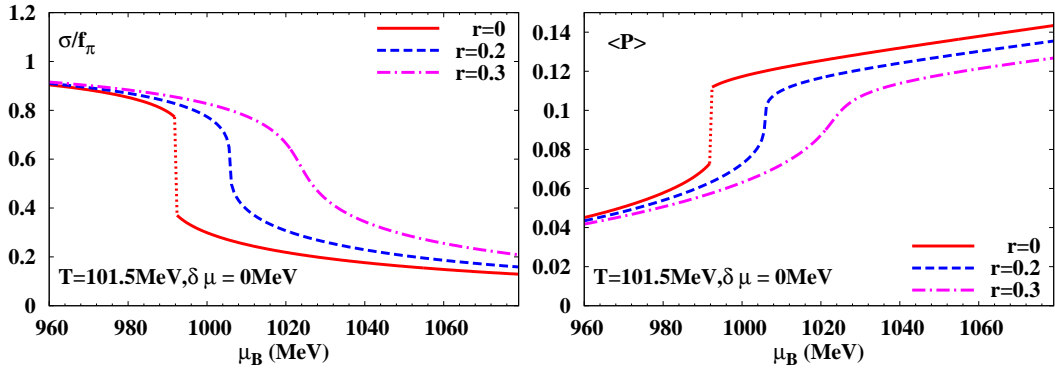


FIG. 2. The order parameters σ (left panel), P (right panel) as functions of baryon chemical potential μ_B at $T = 101.5 \text{ MeV} = T_{CP}(\delta\mu = 0 \text{ MeV}, r = 0.2)$ and $\delta\mu = 0 \text{ MeV}$ for several values of the vector-scalar coupling ratio $r = 0, 0.2, 0.3$.

sider dimensionless susceptibility. Figure 3 shows the chiral susceptibility as a function of temperature for several baryon chemical potentials at $\delta\mu = 0 \text{ MeV}$. For each μ_B , we find a peak in χ_σ , where the chiral phase transition occurs. At CP, $(T, \mu_B) = (T_{CP}, \mu_{CP})$, this quantity is divergent which signals a second order phase transition. The critical points are found to be $(T_{CP}, \mu_{CP}) = (117, 975) \text{ MeV}$ at $\delta\mu = 0$ without vector coupling $r = 0$.

As for the case of the chiral transition, the deconfinement transition is a crossover for finite quark masses, and we need to specify a criterion to identify the deconfinement phase boundary. Several prescriptions to define the critical temperature for deconfinement have been used in the literature: the temperature at which the Polyakov loop susceptibility, χ_P , is maximum; the temperature at which dP/dT is maximum [30, 31]; finally, the half-value prescription, in which one identifies the deconfinement temperature with the average of the temperatures at which at $P = 1/2$ and $\bar{P} = 1/2$ [29] (the two differ at finite μ). The Polyakov loop susceptibility χ_P may have a double peak structure in some cases [13]: one peak is related to the chiral phase transition and the other is related to the transition caused by the Polyakov loop mean

field potential. A similar double peak behavior is found in dP/dT [30, 31]. Thus it is not easy to unambiguously define the deconfinement temperature from the Polyakov loop susceptibility or the temperature derivative. Since the Polyakov loop is small ($P, \bar{P} \simeq 0$) in confined phase and large ($P, \bar{P} \simeq 1$) in deconfined phase, the half-value prescription is the simplest one to adopt. Therefore, we adopt the half-value prescriptions to define the deconfinement temperature.

We show the QCD phase boundaries for several $\delta\mu$ values in Fig. 4. The hadron phase shrinks a little and the critical point temperature T_{CP} decreases with increasing $\delta\mu$, while the confinement-deconfinement phase boundary only weakly depends on $\delta\mu$. The reduction of the transition chemical potential may be understood as the density effects. For a simple estimate, let us consider the low T transition in the chiral limit without the vector coupling, where the sum of u and d quark number densities in the chiral restored phase is proportional to $(\mu + \delta\mu)^3 + (\mu - \delta\mu)^3 = 2\mu^3(1 + 3\delta\mu^2/\mu^2)$ as in the free massless case. If the QCD phase transition at finite $\delta\mu$ occurs at the same density in the Wigner phase as that for $\delta\mu = 0$, the transition quark chemical potential is calculated to be $\mu \simeq \mu_c - \delta\mu^2/\mu_c$, where μ_c represents the transition

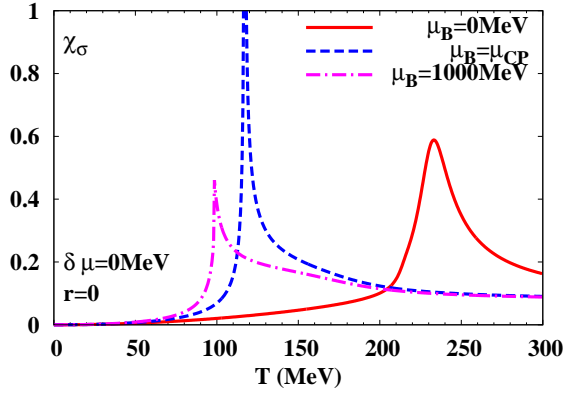


FIG. 3. The chiral susceptibility χ_σ as a function of temperature for different isospin chemical potential $\mu_B = 0$ (solid line), μ_{CP} (dash line), 1000 MeV (dash-dot line) at $\delta\mu = 0$ MeV. χ_σ is divergent at the critical end point.

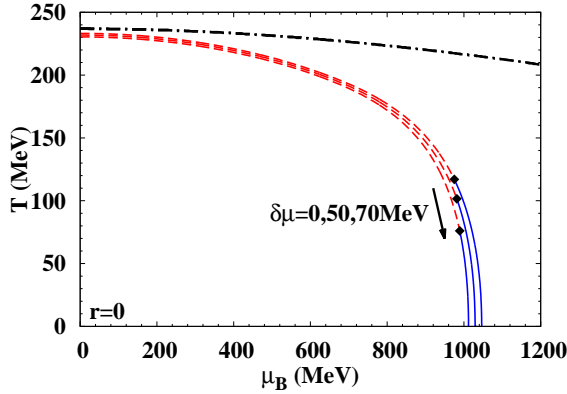


FIG. 4. The QCD phase diagrams for several isospin chemical potential. The red dash and the blue solid lines show the crossover and first order chiral phase transition boundaries respectively at $\delta\mu = 0, 50, 70$ MeV. The square dots show the CP. The black dash-dotted lines show the confinement-deconfinement phase boundaries at $\delta\mu = 0, 70$ MeV.

chemical potential at $\delta\mu = 0$. This estimate gives the transition chemical potential shifts of 7.2 and 14 MeV for $\delta\mu = 50$ and 70 MeV, respectively, which is comparable to the PQM results, 7.0 and 13 MeV. Another possible explanation is the decrease of the effective number of flavors. At finite $\delta\mu$, one of the u or d quarks is favored, and the phase diagram is expected to be closer to that at $N_f = 1$, where the phase transition is weaker.

We note that the deconfinement transition temperature (T_d) is a little higher than the chiral transition temperature T_c . The present behavior is consistent with the lattice Monte-Carlo simulation results, which suggest $T_d > T_c$ [33]. It should be noted that this order depends on the choice of T_0 and is different from some of the effective model results [32]. While the order of T_d and T_c at $\mu = 0$ is an interesting problem on the relation of deconfinement and chiral transitions, it is irrel-

evant to our conclusion and we choose $T_0 = 270$ MeV in the later discussion.

It should be noted that the deconfinement phase boundary is almost insensitive to the baryon chemical potential, leading to a splitting of the chiral and deconfinement transition boundaries. This behavior is similar to the strong coupling lattice QCD results including finite coupling and Polyakov loop effects [31], but it is different from the results obtained from the functional renormalization group method starting from the PQM initial condition at large cutoff [34].

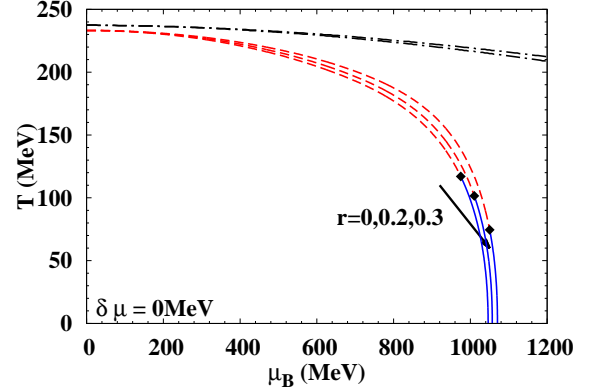


FIG. 5. The QCD phase diagrams for several quark-vector meson couplings. The red dash and blue solid lines show the crossover and first order chiral phase transition boundaries respectively at $r = 0, 0.2, 0.3$. The black dash-dotted lines show the confinement-deconfinement phase boundaries at $r = 0$ and $r = 0.2$.

Figure 5 shows the QCD phase diagrams of symmetric matter ($\delta\mu = 0$) for several quark-vector meson couplings. With increasing vector coupling, the chiral phase boundary moves to the higher μ_B direction, and the CP moves to the higher μ_B and lower T direction. The behavior of μ_{CP} is understood from the effective μ_B shift. We can ignore the ρ^0 meson effects in symmetric matter, and the effective chemical potential is given as $\tilde{\mu} = \mu - rg\omega$. Therefore, a strong vector interaction makes $\tilde{\mu}$ small for a given μ_B [35], and the phase boundaries and the CP moves to high μ_B for finite vector coupling, $r \neq 0$. By comparison, the vector coupling dependence of the confinement-deconfinement phase boundary is small.

We show the QCD phase diagram in $(T, \mu_B, \delta\mu)$ space in Fig. 6. As already mentioned, $\delta\mu$ reduces T_{CP} and the transition baryon chemical potential at $T = 0$. Then the first order boundary narrows with increasing $\delta\mu$, and eventually the CP disappears at a certain value of $\delta\mu$. This happens also for the NJL model, as we discuss in more detail in the Appendix. This behavior is important when we consider the chiral phase transition in dense and isospin asymmetric matter, which is realized in the core of neutron stars, where $\delta\mu$ becomes large. For example, the reduced CP temperature may affect the dynamical black hole (BH) formation processes. The highest temperature during the BH formation is calculated to be $T \sim 70$ MeV, and compressed matter may experience either the first order, crossover, or CP sweep depending on the CP location in asymmetric matter [6].

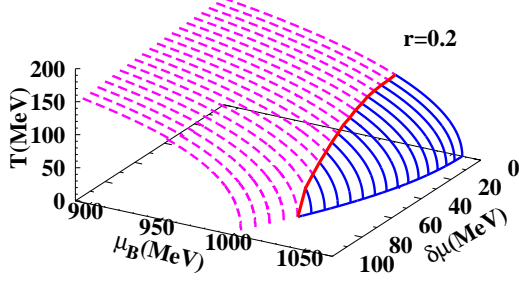


FIG. 6. The 3-dimensional $(T, \mu_B, \delta\mu)$ QCD phase diagram in PQM with $r = 0.2$. The dash lines and the blue solid lines show the crossover and first order chiral phase boundary respectively. The red solid line shows CP for different $\delta\mu$.

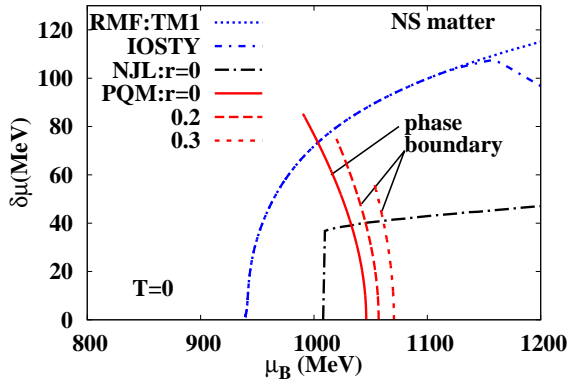


FIG. 7. This figure shows the first order phase boundaries at $T = 0$ in PQM model with $r = 0$ (red solid line), 0.2 (red dash line) and 0.3 (red dot line) and $(\mu_B, \delta\mu)$ for neutron star matter calculated by NJL [39] with $r = 0$ (black dash-dot line), TM1 [36] (blue dot line) and IOSTY [37] (blue dash-dot line) [25].

Another example of dense asymmetric matter is the neutron star core. In the neutron star core, the internal temperature is of the order of $10^6 \text{ K} \sim 10^{-4} \text{ MeV}$, which is small enough compared with the Fermi energy of neutrons. The baryon density would reach a few times of the nuclear density, $\sim 10^{15} \text{ g/cm}^3$. Since the neutron density is much larger than the proton density, the isospin chemical potential, $\delta\mu = (\mu_n - \mu_p)/2 = (\mu_d - \mu_u)/2$, is finite and large. In relativistic mean field (RMF) models, $\delta\mu$ is calculated to reach 100 MeV in the neutron star core. Thus we can regard the neutron star core matter as asymmetric matter at zero temperature.

In Fig. 7, we compare the first order phase transition boundary in PQM and β equilibrium line in RMF at $T = 0$ [25]. Here we show the boundary for several values of r . RMF parameter sets of TM1 [36] and IOSTY [37] are adopted as typical examples. TM1 is a model which describes bulk prop-

erties of normal and neutron rich nuclei as well as the nuclear matter saturation point. IOSTY is an extended version of TM1, which includes degrees of freedom of nucleons and hyperons. This comparison shows that for $r = 0.2$ and 0.3 , large $\delta\mu$ makes the chiral transition in neutron star crossover. In IOSTY, hyperons are calculated to appear at $\mu_B \simeq 1100 \text{ MeV}$, then the transition to quark matter occurs before hyperons appear. Since the first order transition generally makes the equation of state softer at around the transition density, the crossover nature may help to keep the EOS stiff enough and to support the heavy neutron stars [38].

We also compare the phase boundary at $T = 0$ with those in flavor SU(3) NJL model results of the neutron star matter [39]. Since constituent quark mass in Ref. [39] is different from that of the present work, we show their results with shifted μ_B . We find that NJL shows small $\delta\mu$ values around the transition. This difference mainly comes from the isovector coupling with quarks and nucleons. In quark matter, we have chosen the vector coupling in the range $0 \leq r \leq 0.3$. In nuclear matter, isovector-vector coupling is chosen to reproduce binding energies of neutron rich nuclei, and it corresponds to $r \simeq 1.0 \sim 1.2$. Thus $\delta\mu$ is calculated to be larger in nuclear matter.

IV. SUMMARY

We have investigated the QCD phase transition in isospin asymmetric matter using the Polyakov loop extended quark meson (PQM) model. Specifically, we have discussed isospin chemical potential $\delta\mu$ and quark-vector meson coupling dependence of the QCD phase boundaries. In PQM, we show $\delta\mu$ reduces the temperature of the QCD critical point, and for large $\delta\mu$, the critical point is found to disappear. We also show the finite quark-vector meson coupling shifts the chiral phase boundary to higher baryon chemical potential and reduces the temperature of the CP. This scenario is in agreement with the one obtained within other chiral models [6, 39].

We have also discussed the order of the chiral phase transition in neutron stars from the comparison of the QCD phase diagram in PQM and the β equilibrium line in RMF. In neutron stars, $\delta\mu$ is large, then the temperature of the CP becomes lower. Therefore the chiral phase transition may be crossover, even if the transition in symmetric matter ($\delta\mu = 0$) is the first order. In this study, however, we use $(\mu_B, \delta\mu)$ values on the β equilibrium line in neutron star matter calculated with RMF models which do not include the QCD phase transition effects. In order to discuss the QCD phase transition in compact astrophysical phenomena more precisely, we need the EOS which includes both baryonic and quark degrees of freedom.

One may consider the reduction of T_{CP} shown in this paper would contradict to the finite lepton-number chemical potential result [24], which suggests the insensitivity of T_{CP} as a function of the lepton-number chemical potential. Their results correspond to the $\delta\mu$ range $\delta\mu \lesssim 40 \text{ MeV}$, while we find that the shift of T_{CP} is large in the range $\delta\mu \gtrsim 50 \text{ MeV}$. Thus their results could be consistent with ours.

The phase diagram structure shown in this article is based

on the assumption that the s -wave pion condensation is not realized in dense baryonic matter. This assumption is consistent with the functional renormalization group calculation [23] and s -wave πN repulsion arguments [25], while the results are not in agreement with the mean field results of PNJL at finite $\delta\mu$ [22]. As a future work, it is an interesting problem to discuss the p -wave pion condensation, the inhomogeneous chiral condensate, and the color superconductor phases in the three-dimensional thermodynamic variable space, $(T, \mu, \delta\mu)$.

ACKNOWLEDGMENTS

T.N. and H.U. are supported by Grants-in-Aid for the Japan Society for Promotion of Science(JSPS) Research Fellows (Nos. 22-3314 and 25-2148). This work was supported in part by Grants-in-Aid for Scientific Research from the Japan Society for the Promotion of Science (JSPS) (Nos. 23340067, 24340054, 24540271 10J03314), by Grant-in-Aid for Innovative Areas from the Ministry of Education, Culture, Sports, Science and Technology of Japan (MEXT) (Area No. 2404, Nos. 24105001, 24105008), by the Yukawa International Program for Quark-Hadron Sciences, and by a Grant-in-Aid for the global COE program “The Next Generation of Physics, Spun from Universality and Emergence” from MEXT.

Appendix A: Critical point within the NJL model at zero temperature

In the main body of this article we have discussed the effect of an imbalance of the chemical potentials of u and d quarks on the location of the critical point (CP) of the QCD phase diagram. Our argument was based mainly on numerical results obtained within the PQM model. We found that finite $\delta\mu$ moves CP towards a smaller chemical potential and a lower temperature. Therefore, we might expect that a large enough $\delta\mu$ causes CP to hit the $T = 0$ plane, then disappearing from the phase diagram. In this Appendix we discuss the same topic within the NJL model. We limit ourselves to consider a system of u and d quarks in the chiral limit: this simplifies the calculations, and allows to identify unambiguously the location of the chiral phase transition in the phase diagram. Our purpose is to show analytically how finite $\delta\mu$ induces a softening of the chiral phase transition at finite μ , pushing the CP to lower values of temperature (and baryon chemical potential). Eventually, for large enough $\delta\mu$ the CP hits the $T = 0$ plane. For the purpose of our discussion it is therefore enough to consider the system at $T = 0$ and study the change of the order of the chiral phase transition at finite μ .

The thermodynamic potential of the NJL model at zero temperature can be written as [10]

$$\Omega = \frac{\sigma^2}{G} - 2N_c N_f \int \frac{d\mathbf{p}}{(2\pi)^3} E_p + 2N_c \sum_f \int \frac{d\mathbf{p}}{(2\pi)^3} (E_p - \mu_f) \Theta(\mu_f - E_p), \quad (\text{A1})$$

where $E_p = \sqrt{\mathbf{p}^2 + M^2}$ with $M = 2\sigma = -4G\langle\bar{q}_f q_f\rangle$. Here G corresponds to the 4-fermion NJL coupling constant, and in agreement with the notation of the main text we have put $\mu_u = \mu - \delta\mu$ and $\mu_d = \mu + \delta\mu$. The last addendum on the r.h.s. of the above equation corresponds to the valence quarks contributions. The vacuum part is regularized by cutting the momentum integral at the scale $|\mathbf{p}| = \Lambda$.

Our strategy is as follows: we perform a Ginzburg-Landau expansion of the effective potential,

$$\Omega = \frac{\alpha_2}{2}\sigma^2 + \frac{\alpha_4}{4}\sigma^4 + \frac{\alpha_6}{6}\sigma^6, \quad (\text{A2})$$

where we have subtracted an irrelevant term which does not depend on the condensate. At zero temperature and finite chemical potential the coefficients are easily determined from an expansion of Eq. (A1) around $\sigma = 0$. We get

$$\alpha_2 = \frac{2}{G} - \frac{4N_c}{\pi^2}\Lambda^2 + \frac{2N_c}{\pi^2}(\mu_u^2 + \mu_d^2), \quad (\text{A3})$$

$$\alpha_4 = -\frac{48N_c}{\pi^2} \left(2 - \log \frac{\Lambda^2}{\mu_u \mu_d} \right), \quad (\text{A4})$$

$$\alpha_6 = \frac{480N_c}{\pi^2} \left(\frac{1}{\mu_u^2} + \frac{1}{\mu_d^2} \right). \quad (\text{A5})$$

We notice that $\alpha_6 > 0$ causing the potential to be bounded from below. As a consequence it is possible to study the phase transition studying the signs of the first two coefficients. The phase transition is of first (second) order if $\alpha_4 < 0$ ($\alpha_4 > 0$). At the critical point, where the first and second order transition lines meet, one has $\alpha_2 = \alpha_4 = 0$. Solving $\alpha_2 = 0$ leads to a relationship between μ and $\delta\mu$; using the solution of the latter in the equation $\alpha_4 = 0$ leads to the critical value of $\delta\mu \equiv \delta\mu_c$ at which the CP hits the $T = 0$ plane, namely

$$\delta\mu_c^2 = -\frac{\pi^2}{2GN_c N_f} + \Lambda^2 \left(\frac{1 - e^{-2}}{2} \right) \quad (\text{A6})$$

Using the standard parameters of the model [10] we find $\delta\mu_c \approx 140$ MeV. This result shows that finite $\delta\mu$ changes the order of the chiral phase transition at zero temperature and finite chemical potential.

The fact that finite $\delta\mu$ leads to the softening of the phase transition can be grasped from Eq. (A4); in fact, for $\delta\mu \ll \mu$ one has

$$\alpha_4 \approx \alpha_4(\delta\mu = 0) + \frac{48N_c}{\pi^2} \frac{\delta\mu^2}{\mu^2}; \quad (\text{A7})$$

the above equation shows that $\delta\mu \neq 0$ makes α_4 less negative, thus favoring a second order phase transition. The same conclusion can be drawn by using an extended version of the GL analysis including derivative terms [40].

-
- [1] See for example, P. Haensel, A. Y. Potekhin and D. G. Yakovlev, (Astrophysics and space science library 326).
- [2] T. Hatsuda, *Mod. Phys. Lett. A* **2**, 805 (1987); I. Sagert *et al.*, *Phys. Rev. Lett.* **102**, 081101 (2009).
- [3] K. Sumiyoshi, S. Yamada, H. Suzuki and S. Chiba, *Phys. Rev. Lett.* **97**, 091101 (2006).
- [4] K. Sumiyoshi, S. Yamada and H. Suzuki, *Astrophys. J.* **667**, 382 (2007).
- [5] K. Sumiyoshi, C. Ishizuka, A. Ohnishi, S. Yamada and H. Suzuki, *Astrophys. J. Lett.* **690**, 43 (2009).
- [6] A. Ohnishi, H. Ueda, T. Z. Nakano, M. Ruggieri and K. Sumiyoshi, *Phys. Lett. B* **704**, 284 (2011).
- [7] F. Karsch, *Lect. Notes Phys.* **583**, 209 (2002).
- [8] J. Greensite, *Prog. Part. Nucl. Phys.* **51**, 1 (2003).
- [9] Z. Fodor and S. D. Katz, *JHEP* **0203**, 014 (2002); S. Ejiri, C. R. Allton, S. J. Hands, O. Kaczmarek, F. Karsch, E. Laermann and C. Schmidt, *Prog. Theor. Phys. Suppl.* **153**, 118 (2004); R. V. Gavai and S. Gupta, *Phys. Rev. D* **71**, 114014 (2005); P. de Forcrand, S. Kim and O. Philipsen, *PoS LAT2007*, 178 (2007); P. de Forcrand and O. Philipsen, *JHEP* **0811**, 012 (2008).
- [10] Y. Nambu and G. Jona-Lasinio, *Phys. Rev.* **122**, 345 (1961); *ibid.* **124**, 246 (1961); U. Vogl and W. Weise, *Prog. Part. Nucl. Phys.* **27**, 195 (1991); S. P. Klevansky, *Rev. Mod. Phys.* **64**, 649 (1992); T. Hatsuda and T. Kunihiro, *Phys. Rept.* **247**, 221 (1994); M. Buballa, *Phys. Rept.* **407**, 205 (2005).
- [11] D. U. Jungnickel and C. Wetterich, *Phys. Rev. D* **53**, 5142 (1996).
- [12] P. N. Meisinger and M. C. Ogilvie, *Phys. Lett. B* **379**, 163 (1996).
- [13] K. Fukushima, *Phys. Lett. B* **591**, 277 (2004).
- [14] C. Ratti, M. A. Thaler and W. Weise, *Phys. Rev. D* **73**, 014019 (2006); S. Rossner, C. Ratti and W. Weise, *Phys. Rev. D* **75**, 034007 (2007); C. Sasaki, B. Friman and K. Redlich, *Phys. Rev. D* **75**, 074013 (2007).
- [15] B. J. Schaefer, J. M. Pawłowski and J. Wambach, *Phys. Rev. D* **76**, 074023 (2007).
- [16] V. Skokov, B. Friman, E. Nakano, K. Redlich and B. J. Schaefer, *Phys. Rev. D* **82**, 034029 (2010).
- [17] M. A. Stephanov, *PoS LAT2006*, 024 (2006).
- [18] B. Mohanty [STAR Collaboration], *J. Phys. G* **38**, 124023 (2011) [arXiv:1106.5902 [nucl-ex]]; J. T. Mitchell [PHENIX Collaboration], arXiv:1211.6139 [nucl-ex].
- [19] M. A. Stephanov, K. Rajagopal and E. V. Shuryak, *Phys. Rev. Lett.* **81**, 4816 (1998); D. T. Son and M. A. Stephanov, *Phys. Rev. D* **70**, 056001 (2004); H. Fujii, *Phys. Rev. D* **67**, 094018 (2003); M. A. Stephanov, *Phys. Rev. Lett.* **102**, 032301 (2009); Y. Minami and T. Kunihiro, *Prog. Theor. Phys.* **122**, 881 (2010); M. A. Stephanov, K. Rajagopal and E. V. Shuryak, *Phys. Rev. D* **60**, 114028 (1999).
- [20] R. Oechslin and H. -T. Janka, *Phys. Rev. Lett.* **99**, 121102 (2007); L. Baiotti, B. Giacomazzo and L. Rezzolla, *Phys. Rev. D* **78**, 084033 (2008); K. Kiuchi, Y. Sekiguchi, M. Shibata and K. Taniguchi, *Phys. Rev. Lett.* **104**, 141101 (2010); K. Hotokezaka, K. Kyutoku, H. Okawa, M. Shibata and K. Kiuchi, *Phys. Rev. D* **83**, 124008 (2011).
- [21] H. Abuki, M. Ciminale, R. Gatto, N. D. Ippolito, G. Nardulli and M. Ruggieri, *Phys. Rev. D* **78**, 014002 (2008); H. Abuki, R. Anglani, R. Gatto, G. Nardulli and M. Ruggieri, *Phys. Rev. D* **78**, 034034 (2008);
- [22] T. Sasaki, Y. Sakai, H. Kouno and M. Yahiro, *Phys. Rev. D* **82**, 116004 (2010); J. O. Andersen and L. Kyllingstad, *J. Phys. G* **37**, 015003 (2009).
- [23] K. Kamikado, N. Strodthoff, L. von Smekal and J. Wambach, *Phys. Lett. B* **718**, 1044 (2013).
- [24] S. B. Ruster, V. Werth, M. Buballa, I. A. Shovkovy and D. H. Rischke, *Phys. Rev. D* **73**, 034025 (2006).
- [25] A. Ohnishi, D. Jido, T. Sekihara and K. Tsubakihara, *Phys. Rev. C* **80**, 038202 (2009).
- [26] M. Kitazawa, T. Koide, T. Kunihiro and Y. Nemoto, *Nucl. Phys. A* **721**, 289 (2003); Z. Zhang and T. Kunihiro, *Phys. Rev. D* **80**, 014015 (2009); O. Lourenco, M. Dutra, T. Frederico, A. Delfino and M. Malheiro, *Phys. Rev. D* **85**, 097504 (2012).
- [27] G. Boyd, J. Engels, F. Karsch, E. Laermann, C. Legeland, M. Lutgemeier and B. Petersson, *Nucl. Phys. B* **469**, 419 (1996).
- [28] K. Fukushima, *Phys. Lett. B* **695**, 387 (2011).
- [29] T. Kahara and K. Tuominen, *Phys. Rev. D* **82**, 114026 (2010).
- [30] T. Kahara and K. Tuominen, *Phys. Rev. D* **78**, 034015 (2008).
- [31] K. Miura, T. Z. Nakano, A. Ohnishi and N. Kawamoto, arXiv:1106.1219 [hep-lat]; T. Z. Nakano, K. Miura and A. Ohnishi, *Phys. Rev. D* **83**, 016014 (2011) [arXiv:1009.1518 [hep-lat]].
- [32] B. -J. Schaefer, M. Wagner and J. Wambach, *Phys. Rev. D* **81**, 074013 (2010) [arXiv:0910.5628 [hep-ph]].
- [33] Y. Aoki, Z. Fodor, S. D. Katz and K. K. Szabo, *Phys. Lett. B* **643**, 46 (2006); S. Ejiri *et al.* [WHOT-QCD Collaboration], *Phys. Rev. D* **82**, 014508 (2010); M. Cheng, N. H. Christ, M. Li, R. D. Mawhinney, D. Renfrew, P. Hegde, F. Karsch and M. Lin *et al.*, *Phys. Rev. D* **81**, 054510 (2010); A. Bazavov *et al.* [HotQCD Collaboration], *J. Phys. G* **38**, 124099 (2011).
- [34] B. -J. Schaefer, J. M. Pawłowski and J. Wambach, *Phys. Rev. D* **76**, 074023 (2007) [arXiv:0704.3234 [hep-ph]]; T. K. Herbst, J. M. Pawłowski and B. -J. Schaefer, *Phys. Lett. B* **696**, 58 (2011) [arXiv:1008.0081 [hep-ph]].
- [35] K. Fukushima, *Phys. Rev. D* **77**, 114028 (2008) [Erratum-ibid. *D* **78**, 039902 (2008)].
- [36] Y. Sugahara and H. Toki, *Nucl. Phys. A* **579**, 557 (1994).
- [37] C. Ishizuka, A. Ohnishi, K. Tsubakihara, K. Sumiyoshi and S. Yamada, *J. Phys. G* **35**, 085201 (2008).
- [38] P. Demorest, T. Pennucci, S. Ransom, M. Roberts and J. Hessels, *Nature* **467**, 1081 (2010).
- [39] H. Abuki, R. Gatto and M. Ruggieri, *Phys. Rev. D* **80**, 074019 (2009).
- [40] Y. Iwata, H. Abuki and K. Suzuki, *AIP Conf. Proc.* **1492**, 293 (2012); H. Abuki, *Phys. Rev. D* **87**, 094006 (2013).